INVESTIGATION OF SMALL SCALE HYDRODYNAMIC PROCESSES USING HIGH RESOLUTION SAR IMAGERY AND ADCP DATA

Olga Lavrova [(1)], Andrey Serebryany [(1, 2)], Tatiana Bocharova [(1)]

[(1)] Space Research Institute of RAS, 84/32 Profsoyuznaya str., Moscow, Russia, Email: olavrova@iki.rssi.ru
[(2)] Andreev Acoustic Institute, 4 Shvernik str., Moscow, Russia, Email: serebryany@hotmail.com

ABSTRACT

Results of experimental work obtained in September-October 2011 and June and September 2012 on the northeastern Black Sea shelf are presented. Transects from the coast to the shelf edge were conducted using acoustic Doppler current profiler (ADCP) in conjunction with radar imaging of the region of experiment from satellites Envisat, Radarsat-2 and TerraSAR-X and optical imaging by Envisat MERIS and Terra/Aqua MODIS.
A large number of anticyclonic and cyclonic small-scale eddies are detected and their characteristics assessed. Special focus is on coastal current reversal events in association with anticyclonic eddies.
Cases of short-period internal waves induced by intense anticyclonic coastal eddies detected based on the ADCP data are discussed.
A heavy rainfall accompanied by massive turbid freshwater outflow into the sea made suspended matter concentration charts compiled from Envisat MERIS data highly informative on the coastal water dynamics, eddy structures in particular.

1. INTRODUCTION

Vortical processes in the northeastern part of the Black Sea have long been the subject of successful studies of Russian scientists from various research organizations such as P.P. Shirshov Institute of Oceanology RAS and its Southern Division, Institute of Applied Physics RAS, N.N. Andreev Acoustics Institute and Space Research Institute RAS [1-3]. The main focus was on mesoscale eddy structures with typical sizes of 30 - 100 km. Recent rapid advances in satellite techniques of observation of ocean surface and increasing accessibility of high resolution data have paved the way to a closer investigation of vortical processes, including those with scales down to hundreds of meters, i.e. less than the internal baroclinic Rossby radius of deformation, which is Rd ≈ 15-20 km in the Black Sea. Such eddy structures, classified as submesoscale, demand considerable research effort. Their formation mechanisms, penetration depth, lifetime span, fine spatial structure and relation to mesoscale eddy structures remain unclear. In radar images, eddies and other vortical elements are manifested through either passive tracers or contrasts in convergence-divergence zones. Passive tracers are primarily films of surfactants known to damp short surface waves and form slicks.

An important question is what stands behind the slick eddy patterns in reality? Is it the eddy fine spatial structure comprised of multiple jets? Similarly to surface patterns of internal waves, in this case slicks appear in zones of converging currents. The widths of slick bands are constrained within the range of 100-300 m, whereas the distance between the bands depend on the scale of an eddy. In submesoscale eddies, the distance seldom exceeds 1 km (Fig. 1).

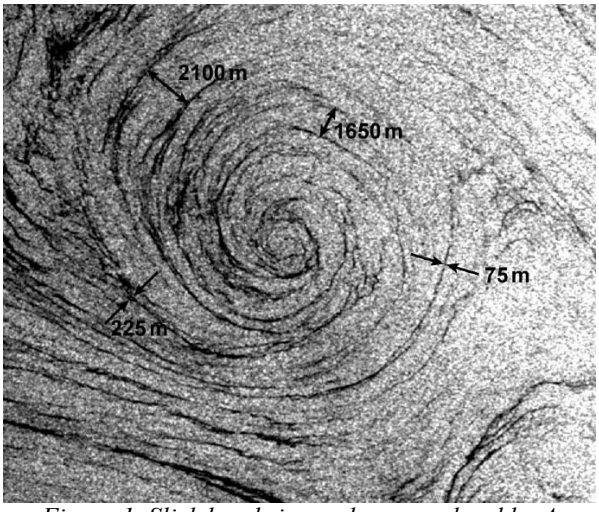

Figure 1. Slick bands in a submesoscale eddy. A fragment of Envisat ASAR image of 10.05.2007 obtained over the northeastern Black Sea [4]

Regular acquisition of high resolution satellite data in various seasons coupled with subsatellite *in-situ* measurements of current parameters may help to clarify at least some of the above issues.

Coastal waters of the Black Sea in the vicinity of the town of Gelendzhik have for a long time been the site of subsatellite experiments, where new devices were tested, regular observations and measurements of different metocean parameters were conducted. This is explained not only by the large number of phenomena and processes of interest, including vortical ones, typical of the region, but also important local applications of such activities. The study of water dynamics is a key element of environmental forecasts for this Russia's largest recreation area on the Black Sea

Proc. 'ESA Living Planet Symposium 2013', Edinburgh, UK
9–13 September 2013 (ESA SP-722, December 2013)

affected by tremendous and ever-growing anthropogenic pressure. Moreover, closely located to Gelendzhik are the two largest Russian ports on the Black Sea, Novorossiisk and Tuapse, with their busy marine traffic. Regular satellite observations in microwave and visible ranges not only provide the opportunity to detect pollution of vast sea surface areas but also to monitor its transport and evolution.

The present paper discusses some results of the experiments conducted in September - October 2011, and June and September 2012 in the northeastern part of the Black Sea near the Gelendzhik coast. The aims of the experiments were to:

- investigate hydrodynamic processes in the region;
- tune operational access to high resolution satellite data;
- estimate the informative value and restrictions of various radar data products;
- investigate the fine spatial structure of currents based on radar and acoustic data;
- identify sea surface processes detected by means of ADCP.

2. STUDY AREA

Subsatellite experiments were conducted in the north-eastern part of the Black Sea in the coastal shelf zone between the Golubaya and Gelendzhik Bays (Fig. 2).

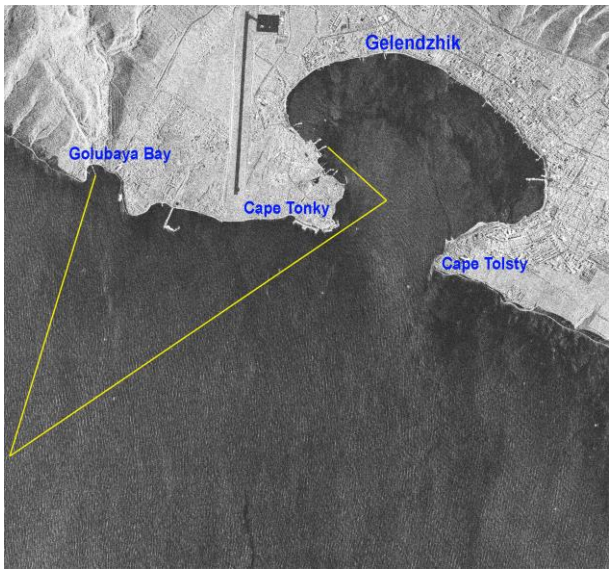

Figure 2. The region of subsatellite measurements. A fragment of TerraSAR-X image of 30.09.2011. The yellow line marks the typical path of the survey boat

The key element of large-scale water circulation in the Black Sea is the cyclonic Rim Current along the Sea's periphery with the flow core located approximately above the continental slope. The width of the shelf zone in the region of the experiments is about 7-8 km [3].

As many-year studies show, the current in the northeastern Black Sea is typically bimodal. Most of the time it is northwestward and coincides with the direction of the Rim Current. Frequently, however, especially in September and October months, the current reverses to southeast. This is commonly presumed to be linked to the passage of small-scale coastal anticyclonic eddies.

3. SUBSATELLITE MEASUREMENT TECHNIQUE AND DATA USED

Subsatellite measurements were conducted in three stages: from 28 September to 14 October 2011, from 4 to 15 June 2012 and from 10 to 29 September 2012. They included:

1. Transects across the shelf from the coastline to the shelf edge by means of Rio Grande 600 kHz acoustic Doppler current profiler (ADCP). This type of ADCP is considered to be useful not only in investigation of currents, but also internal waves, eddies and other dynamic processes in the shelf zone [5]. The measured parameters are current direction and velocity, acoustic backscatter with depth (averaging over depth cells of 0.5 m). The ADCP was mounted aboard of a boat moving steadily at a speed of 2-2.5 m/s.
2. Measurements along the transects across the shelf from the coastline to the shelf edge by means of Valeport miniSVP sound velocity profiler (measures temperature, sound velocity and pressure for further depth calculation). Profiles were registered from the water surface down to the bottom at 7-8 locations along the transect.
3. Long-term (two-week) measurements by a buoy-mounted thermistor set located on a transect line at the depth of 35 m. The set comprised ten Star Oddi Centi temperature sensors that recorded data every 30 s.

Experiments of previous years showed that dynamic processes in the region, the spatial structure of coastal anticyclonic eddies in particular, are best revealed through measurements along "open scissors"-shaped transects; for instance, one transect from the pier in the Golubaya Bay toward the shelf edge and another from the same shelf edge location toward Cape Tonky. A satellite radar image of the study region is presented in (Fig. 2). The yellow line indicates a typical path of the survey boat.

Subsatellite experiments were organized in such a way, that at the time of satellite radar imaging the boat was at the farthest location from the coast, that is at the shelf edge. Therefore, the boat started out to sea 1.5 - 2 hours before the satellite overflight time. At that moment, at the shelf edge location, hydrological measurements were made and afterward the boat sailed toward the Golubaya or Gelendzhik Bays making short stops for measurements. Alongside with the open sea works,

visual observations and camera shooting from coastal vantage points were performed. At the time of satellite overflight, the state of the sea surface was thoroughly examined and documented, including reports on wave development stage, presence of slicks, locations of ships; wind speed and direction were also logged.

Satellite images of the study region were obtained from synthetic aperture radars (SAR) mounted on board Envisat (2011), TerraSAR-X, TanDEM-X and Radarsat-2 satellites. All data, except Envisat, were provided in the framework of the Russian-German project "Detecting and Tracking Small-Scale Eddies in the Black Sea and the Baltic Sea Using High-Resolution Radarsat-2 and TerraSAR-X Imagery" (DTEddie). In total, 31 high resolution images were obtained: 16 Radarsat-2, 13 TerraSAR-X, 2 TanDEM-X along with 5 Envisat ASAR images at a resolution of 150 m.

4. RESULTS

4.1. Manifestation of eddies

Analysis of the data collected during regular campaigns on satellite monitoring of the coastal waters of the Black Sea has shown, that satellite images carry manifestations of a large number of eddies of rather small scale, with diameters of a few to tens of kilometers; sometimes they are accompanied by eddies of even less scale. As a rule, such eddies have a spiral shape. They may appear as solitary eddies, dipoles, eddy chains or eddy clusters. Due to small size, non-stationary character, sudden occurrence and short lifetime, they represent a difficult subject of investigation. The mechanisms for the formation of small-scale eddies in the north-eastern Black Sea are presumed to be wind stress, current shear instability, river outflow, interaction of eddies and their dissipation, interaction of currents with small-scale coastal irregularities (headlands and bays) [1; 3; 6]. Other hypothetical mechanisms for such spiral eddy formation are disturbances and convection in the near-surface atmospheric layer [7].

Analyzing the data obtained during our subsatellite experiments we attempted to:

- determine current speed and direction from ADCP measurements;
- detect countercurrents, whose directions are opposite to that of the Rim Current;
- associate slicks detected in SAR images with countercurrents registered by ADCP and viewed as candidate eddy flows;
- determine the character of current variation with depth;
- register the change of the thermocline position over the eddy passage time.

The third series of subsatellite experiments held in September 2012 is of particular interest. In total, the survey boat went to sea eleven times matching nearly all SAR imaging events. Fig. 3 presents a sequence of ADCP-derived currents along transects made on 10 - 28 September (north and coast are upward).

As is clear from Fig. 3, southeastward currents (countercurrents) were registered on 7 transects. Three times, on 17, 18 and 28 September, the current was observed to shift from southeastward near the coast to northwestward farther off. We have all grounds to attribute these events to the passage of small-scale anticyclonic eddies. Moreover, assuming the eddies are circle-shaped, a rather accurate estimate of their diameters can be made. For instance, the diameter of the 17 September eddy is 8 km. The estimate is based on the assumption that an eddy radius is approximately the distance from the closest point to the coast where the current is southeastward to the point where it reverses direction.

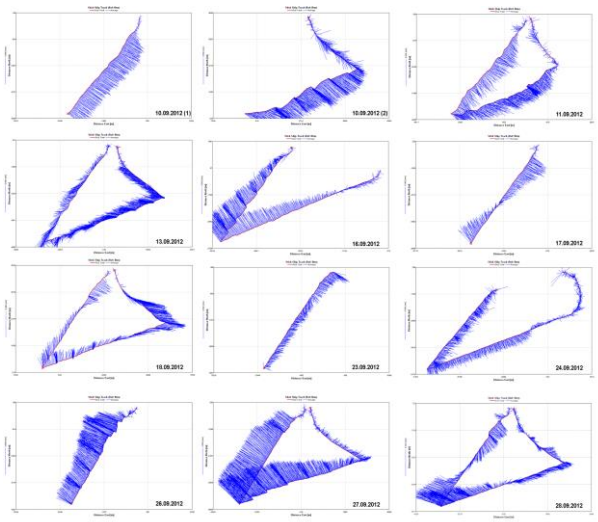

Figure 3. Currents measured by ADCP along the transects on 10 - 28 September 2012

Subsatellite observations conducted over three days on 16 - 18 September provided an insight into the formation and evolution of the 17 September eddy. According to ADCP measurements, on 16 September the character of the current on the whole corresponds to that of the Rim Current being northwestward everywhere, except for a small area adjacent to Cape Tonky where a weak, 0.1 m/s or less, countercurrent is registered. It is noteworthy, that the ADCP-derived location of the current direction reversal coincides with a slick band on SAR data (Fig.4) Within 18 hours, the countercurrent near the coast strengthens up to 0.4 m/s, its velocity gradually decreases to 0 m/s at the distance of about 3 km from the coast, where the current reverses and from this point farther off the coast, its velocity augments up to 0.3 m/s.

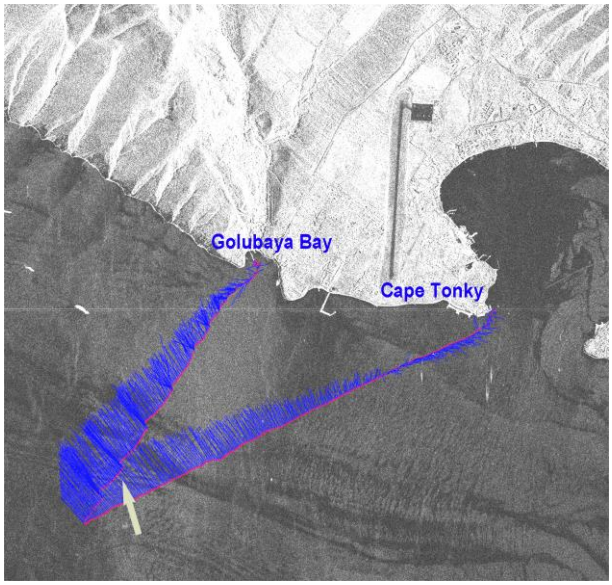

Figure 4. A fragment of TerraSAR-X image on 16.09.2012. Blue vectors indicate current velocity and direction from ADCP data obtained around the time of satellite imaging. The arrow points to the manifestation of internal waves

Notice, that Fig. 3, as well as Fig. 5*a*, shows depth-averaged currents (down to the seasonal thermocline). Variations of current velocity and direction with depth can be analyzed from ADCP velocity magnitude (Fig. 5*b*) and velocity direction (Fig. 5*c*) data. While the current velocity remains approximately the same over the depth, at least down to 20 m, the current direction is fairly constant with depth only at the seaward periphery of the eddy. From the coast seaward, the near-surface current swiftly changes from southeastward to southward, then westward, and, finally, northwestward. The current direction persistent variation with depth initially occurs at the distance of 1.5 km from the coast where the depth is 37 m. Its seaward development has a definite cyclonic character: the direction evolves from southeastward over the depth through mainly eastward, then mainly northward and, finally, to northwestward over the depth. Thus, at the distance of about 3 km, there appears a "zero" point on the ADCP average current data: a weak southward current in the upper layer (depths 0 - 10 m) is counterbalanced by a weak northward current in the lower layer (depths 10 - 20 m).

The character of the current measured the next day, in the morning of 18 September (12 hours after the measurements on 17 September), indicates that the anticyclonic eddy moved southeast, and the boat crossed the rear of the eddy. The current direction is northward down to the depth of 20 m, except for a 1.5 km area adjacent to the coast, where the direction is southeastward.

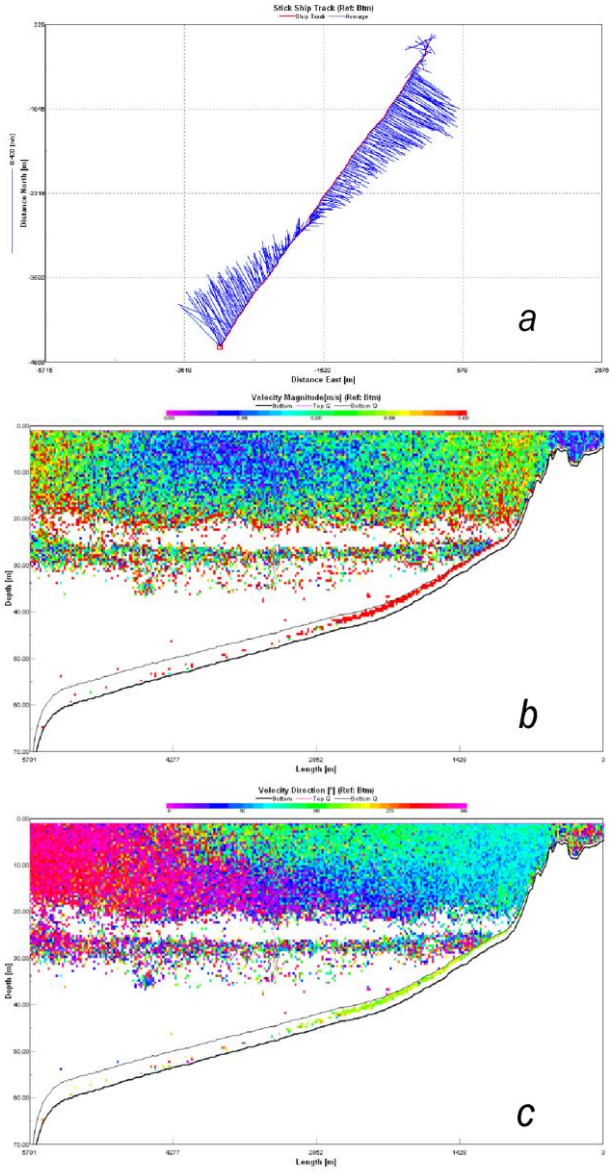

Figure 5. ADCP measurements of anticyclonic eddy parameters along the transect from the coast seaward on 17 September 2012: a) mean current velocity and direction; b) depth distribution of velocity magnitude; c) depth distribution of velocity direction

One further issue is worth consideration. While the overwhelming majority of eddies observed in satellite images are cyclonic eddies [8; 6] visualized by spiral slick patterns, and the northeastern part of the Black Sea is no exception [6], our subsatellite measurements, as a rule, reveal countercurrents associated with the passage of anticyclonic eddies. Leaving aside the intricacies of eddy manifestation in satellite images, we may suggest the following as an explanation. Since our measurements are made from board of a small boat, they are restricted to the 7-8 km coastal zone. Cyclonic eddies cannot be identified in this narrow zone except if their scales do not exceed 5-6 km, because their current direction near the coast coincides with that of the Rim

Current. A good example of current cyclonic meandering, or eventual eddy, is presented in Fig. 6.

Joint analysis of SAR and ADCP data of 13 September reveals a cyclonic eddy of a diameter of 8 km in the study region. In the SAR image it is visualized by spiral-shaped slicks. The ADCP transect lies away from the eddy center, that is why the variation of the current was registered at the distance of 5 km rather than in midway of the 7 km transect.

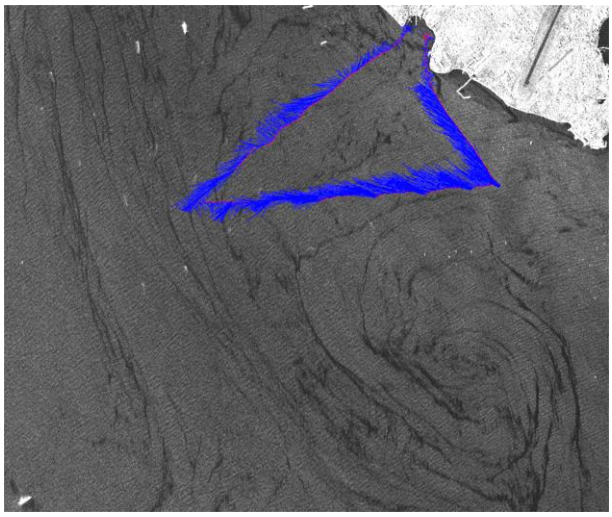

Figure 6. Cyclonic eddy manifested in TanDEM-X image of 13.09.2012. Blue vectors indicate current velocity and direction from ADCP data obtained around the time of satellite imaging

Over the period of the second stage of subsatellite measurements held on 4-15 June 2012, the current field in the northeastern part of the Black Sea was determined by two large vortex structures: an eddy dipole with the anticyclonic component situated to the west of the study region and an anticyclonic eddy to the east. The anticyclonic structures ranging 50-60 km in scale are located as close to each other as 10 km and at a distance of 8-10 km from the coast (Fig. 7). The region of measurements is displaced to the north relative to the area in between the two eddies and lies outside their flows. This hydrodynamic situation causes the coastal current to closer approach the coastline remaining northwestward in the study region. Farther to northwest, the cyclonic flow deflects from the coastline and runs into the area between the mesoscale anticyclonic structures (Fig. 7).

In TerraSAR-X and Radarsat-2 images obtained on 6 June (not presented) with the time difference of 9 minutes, one can easily recognize a wavy slick marking the boundary of the coastal current and a group of slicks delineating the edge of the mesoscale anticyclonic eddy. The mesoscale eddies remained basically quasi-stationary till 9 June, when the dipole moved west, while the anticyclonic eddy nearly dissipated. This caused the Rim Current to deflect from the coastline, weaken and meander, which gave rise to a coastal countercurrent registered on 9 June by ADCP. Later, the newly-formed eddy dipoles did not facilitate meandering of the coastal current and it remained northwestward till the end of the experimental work at that stage. Thus, during the subsatellite experiments in June 2012 no passages of small-scale eddies were detected, except on 9 June.

Figure 7. Vortical structures manifested in the study region on 06.06.2012. A fragment of Terra MODIS true color image. 1 – anticyclonic component of eddy dipole, 2 - anticyclonic eddy, 3 - cyclonic flow

In the course the first stage of subsatellite measurements, in September – October 2011, the current reversal related to small-scale eddy passage was observed twice. These observations will be discussed in detail below in Section 3 devoted to the influence of eddies on the transport of pollutants.

4.2. Manifestation of internal waves

Surface manifestations of internal waves (IW) in the northeastern part of the Black Sea are scarcely detected in satellite data. Over the whole period of 2005-2011, when we conducted regular satellite monitoring of this area based on Envisat ASAR data, only 11 cases of IW were identified [9]. The Black Sea belongs to the class of non-tidal seas, therefore the mechanism of IW generation by tides does not work. Our investigations show that nearly all the instances of IW are located in the immediate vicinity of an eddy edge or hydrologic front. Also they are necessarily accompanied by a sharp and shallow pycnocline.

Several cases of IW manifestation were registered during our subsatellite measurements using ADCP in 2012. IW are recognized in ADCP data by oscillations

of high intensity backscatter layer. Based on these data, it is possible to make fairly accurate estimates of the main IW parameters: amplitudes, wavelengths, as well as their spatial distribution along a transect. For example, a survey of 16 September reveals IW propagating onshore whose wavelengths average 100 m and amplitudes range 8-12 m (Fig. 8). Joint analysis of ADCP and TerraSAR-X data indicates their surface manifestation in the form of three elongated parallel slicks in the radar image (Fig. 4). According to the radar data, the IW wavelength is estimated at 90 m, which is in good agreement with the ADCP data.

Over the two series of measurements in June and September 2012, total six IW packets were registered along the ADCP transects, of which three were also manifested in SAR images. Notice, that their identification in radar images is possible only due to high spatial resolution of TerraSAR-X and Radarsat-2 data. Data logs from the thermistor chain show that at the time of IW propagation, the amplitude of temperature oscillations at the depths of 10 and 15 m sometimes reaches 10° ranging 10°-20°C (Fig. 9). Almost each of the IW instances coincides in time with some eddy situated in close proximity. One may draw a conclusion on the eddy mechanism of IW generation involved.

4.3. Pollutant transport by submesoscale eddies

In the course of subsatellite measurements in 2011 (28 September – 14 October), the sea was closed for several days due to unfavorable weather conditions. That is why the measurements were conducted only on 30 September, 7, 8 and 11 October. Along with persisted strong southward and southwestward wind, it frequently rained, sometimes long and heavily, as a result the rivers were overflown and large quantities of turbid river water discharged into the sea. The color of coastal waters drastically changed and turned greyish, the amount of suspended matter rapidly increased. The downpour occurred on 5 October reached 33 mm and caused not only further increase in river outflows, but evidently also the overflow of the Gelendzhik sewage system tanks situated at Cape Tolsty and sewage discharge into the sea. Accidental discharges from obsolete sewage facilities of Gelendzhik are reportedly a common occurrence [6]. Satellite data also reveal an abrupt rise in suspended matter concentration near Cape Tolsty after the heavy rainfall of 5 October.

The suspended matter concentration chart based on Envisat MERIS data of 7 October shows values exceeding 6 g/m^3 (Fig. 10*a*). Pollutants are carried far away from the accident location trapped by an anticyclonic eddy having the following dimensions: the major axis of 35 km, the minor axis of 16 km. The coastal part of the eddy was registered by the ADCP along a 3.3 km transect in the shelf zone performed to the point with the depth of 35 m (Fig. 10*b*). A rather strong, up to 0.3 – 0.4 m/s, southeastward current was measured in the coastal 1 km zone implying the presence of an anticyclonic eddy of considerable size.

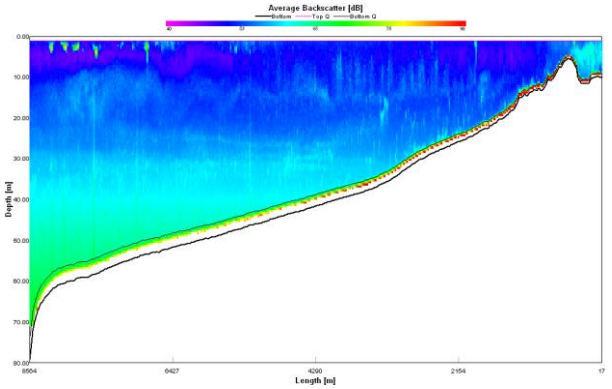

Figure 8. Internal waves manifested in ADCP average backscatter chart of 16.09.2012

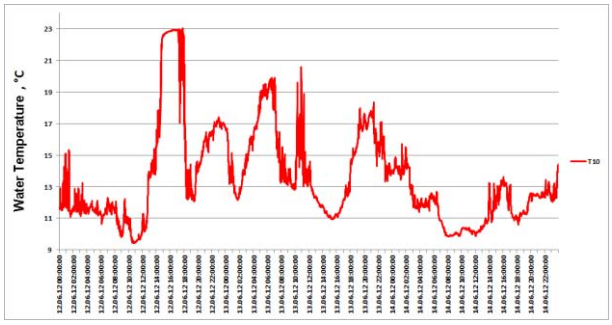

Figure 9. Water temperature timeline over 12, 13 and 14 June 2012 at the depth of 10 m

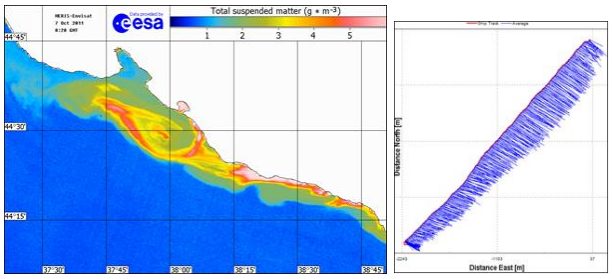

a *b*

Figure 10. Transport of polluted waters under the impact of the anticyclonic eddy on 7 October 2011: a) suspended matter concentration from Envisat MERIS data; b) currents along the ADCP transect; the southeastward direction implies the presence of the anticyclonic eddy

The ADCP data permits to compare volumetric backscatter signals before the rainfall period (survey of 28 September 2011) and after it (survey of 8 October 2011). Fig. 11 presents the corresponding transects measurements. Before the rainfall, the position of the thermocline is quite distinct: it is located at the depth of

20-21 m and divides the water column into two contrasting regions: the upper one with a relatively weak backscatter (backscatter coefficient within 46-50 dB) and the lower one with a significant backscatter (56-59 dB). After the rainfall the situation changes drastically. The position of the thermocline is lower and indistinct, at 22-27 m, while the zone of maximal backscatter (61-67 dB) is shifted upwards to occupy the depths from the sea surface down to 8-10 m and stretches immediately from the coastal area seaward up to the distance of 3 km. Still farther, the high backscatter zone moves deeper reaching 18-20 m and assuming a "patchy" pattern of backscatter coefficient distribution over the transect. Below this zone lies a water layer with backscatter coefficients within 55-57 dB.

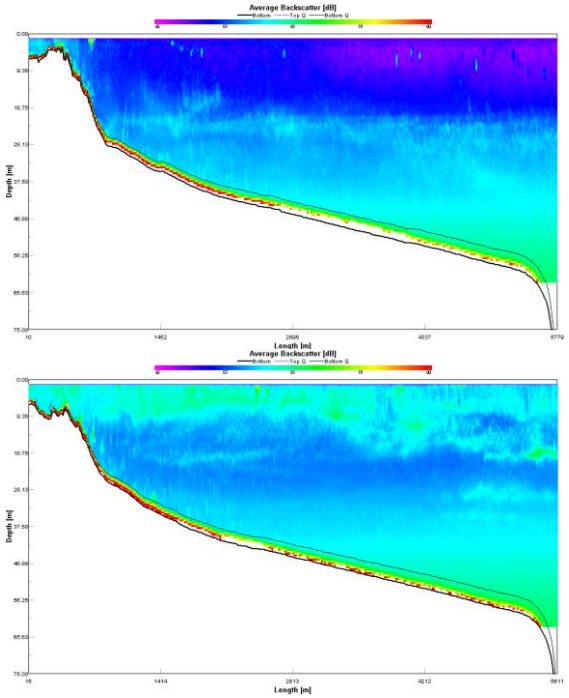

Figure 11. ADCP average backscatter along the across-shelf transects before (28 September, top panel) and after (8 October, bottom panel) the rainfall

In the image acquired by Envisat ASAR on 8 October, the area of polluted waters is distinguished by lower backscatter (dark region) along the coastline near the Gelendzhik and Golubaya Bays and occupies about 60 km^2 (Fig. 12*a*). Meanwhile, considering the suspended matter chart compiled from Envisat MERIS data of 8 October, one can conclude that the polluted waters propagate much more farther away under the impact of the Rim Current (Fig. 12*b*). Of particular interest are the results obtained on 11 October 2011. Two transects were made using the ADCP mounted on the boat. They again have a configuration of "open scissors" with the "pivot" point at the shelf edge. The currents on both transects have basically the same character (Fig. 13*a*). Moving seaward from the coast, one encounters a southeastward current with mean velocity of 0.2 m/s. At the distance of 2.4 km the current slackens and turns clockwise, after that, having changed the direction to northwestward, it strengthens again up to 0.15 m/s at the farthest point. Such character of the current implies the presence of an anticyclonic eddy whose diameter is approximately 10 km.

In situ measurements were conducted simultaneously with high resolution SAR imaging from Radarsat-2 and TerraSAR-X satellites. The time difference between their overpasses was 7 minutes. Four hours later, imaging by the Envisat MERIS sensor was also performed whose data was used to compile the suspended matter concentration chart. A joint analysis of the satellite and *in situ* data shows that the small-scale anticyclonic eddy revealed with the aid of ADCP is part of a larger vortex structure drifting southwest. Maximal measured velocities of the coastal countercurrent coincide with a slick band observed in both SAR images (Fig. 13*a*). The dark region in the vicinity of Cape Tolsty is the evidence that polluted waters still remain near the location of the discharge from municipal sewage facilities.

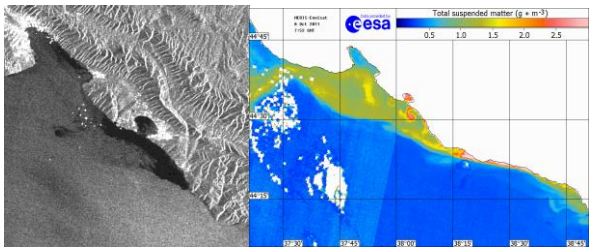

a *b*

Figure 12. Transport of polluted waters on 8 October: a) a fragment of Envisat ASAR image, spatial resolution 150 m. The dark region indicates higher pollution of the sea surface; b) suspended matter concentration from Envisat MERIS data

Comparison of the ADCP and satellite data shows that the area traversed by the southeastward current is characterized by lower concentration, in contrast to the area traversed by the northwestward current and featuring higher concentration of suspended matter flowing from Cape Tolsty (Fig. 13*b*).

5. CONCLUSION

The three series of subsatellite experiments conducted in the northeastern shelf zone of the Black Sea have considerably advanced our understanding of small-scale hydrodynamic processes in the region.

High resolution radar imaging from TerraSAR-X, TanDEM-X and Radarsat-2 along with simultaneous boat surveys using an ADCP operating at a resolution of 0.5 m allowed us to detect six packets of internal waves

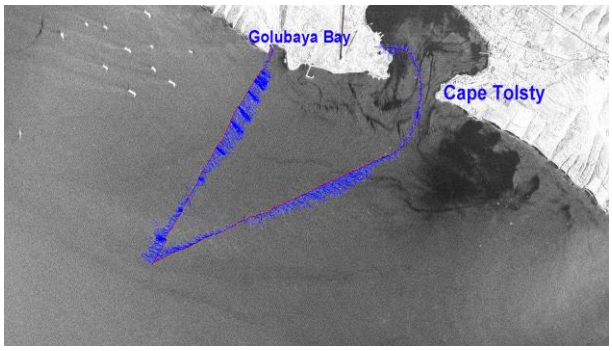

a

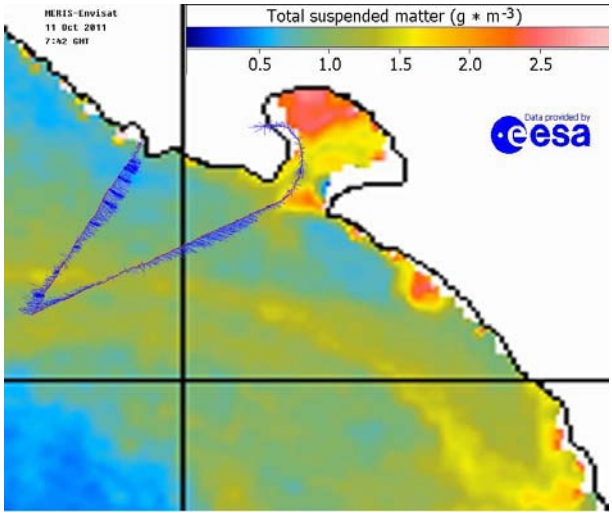

b

Figure 13. The anticyclonic eddy detected on 11 October 2011: a) a fragment of Radarsat-2 image of 11.10.11; b) suspended matter concentration from Envisat MERIS data. Blue vectors indicate current velocity and direction from ADCP data

propagated in the study region. From the ADCP and thermistor data, their amplitudes are estimated to reach 8-10 m. Joint analysis of the SAR data and subsatellite measurement data gives the characteristic wavelength of internal waves to be 90-100 m. It is the satellite data of spatial resolution of 3 m that made it possible to reveal surface manifestations of internal waves of such scale.

The joint analysis of the SAR and acoustic data demonstrates, that a slick is nearly always formed at the interface of two opposing currents, i.e. at the location of coastal current reversal associated with the passage of an anticyclonic eddy.

Our observations in autumn 2011 once again proved, that meso- and submesoscale vortical structures play a significant role in the transport of pollutants. The drift and evolution of water pollution plume from an accidental sewage discharge after a heavy rainfall is tracked both at the surface and through the depth.

6. ACKNOWLEDGMENTS

The work was accomplished with partial financial support of the Russian State Contract # 14.740.12.1342. The Envisat data were obtained in the framework of ESA project C1P6342. Radar data from Radarsat-2, TerraSAR-X were obtained in the framework of SOAR Radarsat-2/TerraSAR-X Project #5074.

7. REFERENCES

1. Ginzburg, A.I., Kostyanoy, A.G., Solov'yev, D.M. & Stanichny, S.V. (2001). Satellite monitoring of eddies and jets in the northeastern Black Sea. *Mapping sciences and remote sensing.* **38**(1), 21-35.

2. Krivosheya, V.G., Moskalenko, L.V. & Titov, V.B. (2004). On the current regime over the shelf near the North Caucasian coast of the Black Sea. *Oceanology.* **44**(3), 331-336.

3. Zatsepin, A.G., Baranov, V.I., Kondrashov, A.A., Korzh, A.O., Kremenetskiy, V.V., Ostrovskii, A.G. & Soloviev, D.M. (2011). Submesoscale eddies at the Caucasian Black Sea shelf and the mechanisms of their generation. *Oceanology.* **51**(4), 592-605.

4. Lavrova, O., Serebryany, A., Bocharova T., Mityagina, M. (2012). Investigation of fine spatial structure of currents and submesoscale eddies based on satellite radar data and concurrent acoustic measurements. Proc. SPIE 8532, Remote Sensing of the Ocean, Sea Ice, Coastal Waters, and Large Water Regions 2012, 85320L.

5. Sabinin, K.D. & Serebryany, A.N. (2012). Results of using acoustic Doppler current profilers for studying the spatial structure of the marine environment. *Acoustical Physics*. **58** (5), 586-595.

6. Lavrova, O.Yu., Kostianoy, A.G., Lebedev, S.A., Mityagina, M.I, Ginzburg, A.I., & Sheremet N.A. (2011). *Complex satellite monitoring of the Russian Seas,* IKI RAS, Moscow, Russia, 470 p.

7. Golitsyn, G.S. (2012). On the nature of spiral eddies on the surface of seas and oceans. *Izvestiya. Atmospheric and Oceanic Physics*. **48**(3), 350-354.

8. Munk, W., Armi, L., Fisher, K. & Zachariasen, F. (2000). Spirals on the sea. Proc. Roy. Soc. 456A, 1217–1280.

9. Lavrova, O. Yu., Mityagina, M. I. & Sabinin, K. D. (2011) Study of internal wave generation and propagation features in non-tidal seas based on satellite synthetic aperture radar data. *Doklady Earth Sciences*, **436**(1), 165–169.